Acta Scientiarum
http://periodicos.uem.br/ojs/acta
ISSN on-line: 1807-8672
Doi: 10.4025/actascitechnol.v47i1.70187

A parallelizable method for two-dimensional wave propagation using subdomains in time with Multigrid and Waveform Relaxation

Maicon Felipe Malacarne[1*], Márcio Augusto Villela Pinto[2] and Sebastião Romero Franco[3]

[1]Departamento de Bioprocessos e Biotecnologia, Associação de Ensino, Pesquisa e Extensão Biopark, Rua Max Planck, Toledo, Paraná, Brazil. [2]Departamento de Engenharia Mecânica, Universidade Federal do Paraná, Curitiba, Paraná, Brazil. [3]Departamento de Matemática, Universidade Estadual do Centro-Oeste, Irati, Paraná, Brazil. *Author for correspondence. E-mail: maicon.unicentro@hotmail.com

ABSTRACT. In this paper we compare the implicit schemes for the solution of the two-dimensional wave equation using Singlegrid and Multigrid methods. The discretization is performed using the Finite Difference Method, weighted in time by an established parameter. The parallelization of the algorithms is ensured by employing the Waveform Relaxation method, where numerical stability is achieved by applying the method of subdomains in time. The primary innovation of this work lies in the development of a high-order method that harnesses the parallelizability and robustness of the Multigrid method, enabling efficient solutions to the 2D wave equation. These methods also effectively mitigate oscillations that would otherwise significantly increase the maximum residual, a concern arising from the application of the standard Waveform Relaxation method.

Keywords: implicit schemes; finite difference method; high-order method and parallel algorithms.

Received on November 1, 2023.
Accepted on April 11, 2024.

Introduction

According to Pierce (1990) the hyperbolic partial differential equation that describes wave propagation is given by,

$$\frac{1}{c^2}\frac{\partial^2 u}{\partial t^2} = \nabla^2 u, \quad (1)$$

where u is the displacement at position over time $t > 0$, for a given constant c associated to the density and the stress field and ∇^2 represents the Laplacian operator. Obtaining reliable, and accurate approximate solutions to the wave equation problem is of paramount importance, being fundamental for understanding problems in acoustics, elastic and electromagnetic phenomena. According to Kocher and Bause (2014), numerical simulation of ultrasonic wave propagation in carbon fiber-reinforced polymers is a relatively new technique that serves damage detection and structural health assessment.

Solving the wave equation for large times in a standard way can be a challenge, which is even greater when trying to perform parallelization of the algorithms (Haut, Babb, Martinsson, Wingate, 2016; Dai & Maday, 2013). A new method, with slightly more stable characteristics, was proposed by Nguyen and Tsai (2020), showing good performance for smooth and constant wave speeds. However, this method proves to be less efficient for problems with discontinuity, in which error propagation occurs during the iterative process.

According to Gander, Halpern, Rannou, and Ryan (2019) although parallelization schemes are successfully applied to diffusion problems, most of them fail when applied to the wave equation, and this is a research topic that should be addressed in more detail. Therefore, these authors proposed a diagonalization scheme with Newmark's method, which proved to be effective for this new class of problems. The authors also performed the application of this procedure to calculate the response of a laminate composite made of Carbon/Epoxy when subjected to an impact load.

In that context, a new method was developed: Waveform Relaxation (WR), which is an iterative method proposed to solve large systems of Ordinary Differential Equations (ODEs), but which can be adapted to time-dependent PDEs. In WR, the spatial domain is decomposed by a set of points, and for each of these points, a

system of ODEs is solved in all time steps (Lelarasmee, Ruehli, & Vincentelli, 1982). A WR method was developed to solve the poroelasticity problem (Franco et al., 2019) which is modeled by a system of parabolic PDEs. Other works that apply parallelization are presented in Bellen and Zennaro (1989) and Chartier and Philippe (1993) for initial value problems and in Keller (1992) for boundary value problems.

To non-steady state problems, the WR algorithms differ from the standard time sweep methods (Time-Stepping) because their iterates are time functions (Gander, 2015). The Partial Differential Equations are transformed into a large set of Ordinary Differential Equations, and an iterative algorithm can be used to solve this system. This numerical solution needs a high computational effort due to the necessity of solving systems of large dimensions at each step point. WR iterations are designed to decouple the original large system into smaller subsystems: in this way, the iteration process can be implemented in a parallel computational environment, since each subsystem can be treated by a single processor (Conte, D'Ambrosio, & Paternoster, 2016).

The instabilities encountered when trying to apply parallelization to hyperbolic problems are also detailed in Ruprecht (2018), where the mathematical theory needed to better understand how these problems arise is explored. A significant contribution is made by noting that for increasing final time or for larger wave numbers, there is an overestimation of the amplitudes that are not damped at the beginning of the process.

Important literature review work on solving partial differential equations (PDEs) using parallelization has been done by Ong and Schroder (2020), in which the authors highlight the importance of developing codes that use methods such as Multigrid, Waveform Relaxation, Subdomains, and Space-Time, as these methods can be employed to increase the degree of parallelization, both spatially and temporally.

The Space Time method was also addressed in Giladi and Keller (2002) for the diffusion and advection problem with domain decomposition using red-black ordering solver, in which high convergence rates were obtained. A variation of the discontinuous Space Time method is proposed in Klaij, Van Der Vegt, and van der Ven (2006), to solve the Navier-Stokes equation using Finite Element Method (FEM), usually this method presents difficulties when working with large deformations in the mesh, but this strategy proved accurate even in these cases.

In Gander and Neumuller (2016) the application of the Multigrid method with Space Time for the heat equation, with discretization using the Finite Element Method in space, was performed, where detailed analyses on convergence and the choice of optimal parameters for total coarsening in time were presented.

The Multigrid method with time reduction (MGRIT) proposed in Falgout, Friedhoff, Kolev, MacLachlan, and Schroder (2014) aims to increase the degree of parallelization of existing algorithms, since it allows for simultaneous spatial and temporal parallelization, because, despite the evolution of data architecture, the processing capacity is limited if only one core is used. This method produces good results, especially if many cores are used.

The MGRIT method as well as other parallelization methods treat the time domain as an extension of the spatial domain. In a simplified way, we can say that this method is based on obtaining approximate solutions on coarse meshes in time, then these solutions can be adopted as initial estimates on more refined meshes and thus the time domain can be divided into subsets, which are solved separately (this process is called F relaxation). This allows parallelization in time to be performed, as in Dobrev, Kolev, Petersson, and Schroder (2017) where an analysis of the convergence of the MGRIT method for two mesh levels is performed.

An important comparison between Multigrid with Space Time, Multigrid with Waveform Relaxation, and MGRIT methods was performed by Falgout et al. (2017) for the diffusion problem. The results showed that all three methods are effective in solving this type of problem, but Multigrid with Space Time has some advantages over MGRIT, especially when a relatively large number of processors are not available.

The Multigrid Method is widespread in literature, having applications to a variety of problems, such as poroelasticity (Franco et al., 2018b; Rodrigues et al., 2022; Franco & Pinto, 2023), diffusive problems (De Oliveira, Franco, & Pinto, 2018; Pinto, Rodrigo, Gaspar, and Oosterlee, 2016), and hyperbolic equations (Malacarne, Pinto, & Franco, 2022). Promising results for the Multigrid method were presented by Franco et al. (2018a) for the heat equation with Space-Time. The authors innovated by proposing a standard form of coarsening, which is based on the degree of anisotropy of the discretized operator. This parameter is calculated using Local Fourier Analysis, resulting in an algorithm with a robust and efficient adaptive smoothing strategy.

Domain Decomposition Methods consist of techniques for solving PDEs where the problem domain can be decomposed into a set of spatial and temporal subdomains, and where parallelization exists when each subdomain is solved independently. Such strategies can be used in various methods, among them are the Finite Difference Method (FDM) and the Finite Element Method (FEM) (Foltyn, Lukas, & Peterek, 2020).

In Ong and Mandal (2018) the Domain Decomposition method combined with the parallelizable Neumann-Neumann and Dirichlet-Neumman Waveform Relaxation methods was used, in which the algorithms were analyzed. The results showed a dependence of the solution on the number of Waveform cycles, which in this case is informed initially, but without a reliable stopping criterion. The main disadvantages of this methodology are the computational effort when the number of Waveform Relaxation cycles is larger than necessary, and the lack of precision of the solution obtained when the number of Waveform Relaxation cycles is insufficient.

In Benedusi, Minion, and Krause (2021) two parallel in time approaches applied to a reaction-diffusion problem were treated. Starting from the continuous time-dependent problem, the methods PFASST (Parallel Full Approximation Scheme in Space and Time) and Multigrid Space Time strategies were compared, where the two showed similar characteristics and results for linear cases, but with a slight advantage when using the PFASST method. For more details on the mathematical formulation of the PFASST method, see Bolten, Moser, and Speck (2017), where Local Fourier Analysis is performed for diffusion and advection problems.

Since obtaining solutions to the wave equation with parallelizable methods is a recurrent theme in literature and of paramount importance, it still presents challenges to be overcome. In this work, we employ the Subdomains in Time method with Waveform Relaxation and compare the results obtained with the Singlegrid and Multigrid methods. Our main innovations are in the reductions of the initial oscillations that exist when applying the standard Waveform Relaxation method and in the improvement of numerical parameters, such as convergence factors and processing time.

Material and methods

In this section we will present the mathematical formulation that describes two- dimensional wave propagation and the discretization using time-weighted Finite Difference Method (FDM). The two-dimensional wave equation can be used to model, for example, the problem of a vibrating rectangular membrane, in which the goal is to find the displacement $u(x, y, t)$, with the independent variables, $0 < x < l_x$ and $0 < y < l_y$, representing the plane's spatial coordinates, at time $t > 0$. Assuming a positive scalar $\alpha^2 = 1/c^2$, that is related to the superficial density and local tension, we define the two-dimensional wave equation (see Olver, 2014) as

$$\frac{\partial^2 u}{\partial t^2} = \alpha^2 \left(\frac{\partial^2 u}{\partial x^2} + \frac{\partial^2 u}{\partial y^2}\right), \tag{2}$$

$$u|_{t=0} = f(x, y), \tag{3}$$

$$\left.\frac{\partial u}{\partial t}\right|_{t=0} = g(x, y), \tag{4}$$

$$u(x, 0, t) = u(x, l_y, t) = u(0, y, t) = u(l_x, y, t) = 0, t > 0, \tag{5}$$

where $f(x, y)$ is the initial setup, $g(x, y)$ is the initial speed and Equation (5) represents the boundary conditions.

Using FDM to discretization and considering the problem defined by Equations. (2) to (5), and a square membrane of side L, that is, $l_x = l_y = L$, we define the size of each spatial element by $h_x = \frac{L}{N_x}$ and $h_y = \frac{L}{N_y}$, and a time increment by $\tau = t_f N_t$, where N_x, N_y and N_t are the numbers of the spatial and temporal intervals, respectively, at time $t_f > 0$. By admitting an approximation $v_{i,j}^k$ for the solution u, at a point of coordinates (x_i, y_j), with time k (see Figure 1), and using implicit discretization in time and central difference in space, the two-dimensional problem can be discretized, expanding the methodology employed for the one-dimensional case (for more details, see Malacarne, Pinto and Franco, 2022). Thus, we have

$$\frac{v_{i,j}^{k-1} - 2v_{i,j}^k + v_{i,j}^{k+1}}{\tau^2} - \frac{\tau^2}{12}\frac{\partial^4 v_{i,j}}{\partial t^4} - \cdots = \tag{6}$$

$$\eta\left(\frac{\left(v_{i-1,j}^{k+1} - 2v_{i,j}^{k+1} + v_{i+1,j}^{k+1}\right)}{h_x^2} - \frac{h_x^2}{12}\frac{\partial^4 v_{i,j}^{k+1}}{\partial x^4} - \cdots\right)$$

$$+\alpha^2(1 - 2\eta)\left(\frac{\left(v_{i-1,j}^{k} - 2v_{i,j}^{k} + v_{i+1,j}^{k}\right)}{h_x^2} - \frac{h_x^2}{12}\frac{\partial^4 v_{i,j}^{k}}{\partial x^4} - \cdots\right)$$

$$+\alpha^2\eta\left(\frac{\left(v_{i-1,j}^{k-1}-2v_{i,j}^{k-1}+v_{i+1,j}^{k-1}\right)}{h_x^2}-\frac{h_x^2}{12}\frac{\partial^4 v_{i,j}^{k-1}}{\partial x^4}-\cdots\right)$$

$$+\alpha^2\eta\left(\frac{\left(v_{i-1,j}^{k+1}-2v_{i,j}^{k+1}+v_{i+1,j}^{k+1}\right)}{h_y^2}-\frac{h_y^2}{12}\frac{\partial^4 v_{i,j}^{k+1}}{\partial y^4}-\cdots\right)$$

$$+\alpha^2(1-2\eta)\left(\frac{\left(v_{i-1,j}^{k}-2v_{i,j}^{k}+v_{i+1,j}^{k}\right)}{h_y^2}-\frac{h_y^2}{12}\frac{\partial^4 v_{i,j}^{k}}{\partial y^4}-\cdots\right)$$

$$+\alpha^2\eta\left(\frac{\left(v_{i-1,j}^{k-1}-2v_{i,j}^{k-1}+v_{i+1,j}^{k-1}\right)}{h_y^2}-\frac{h_y^2}{12}\frac{\partial^4 v_{i,j}^{k-1}}{\partial y^4}-\cdots\right)$$

where η is a weighting parameter, being responsible for weighing the influence of each direction. This process of spatial and temporal discretization is applied in symmetric and orthogonal grids, as illustrated in Figure 1.

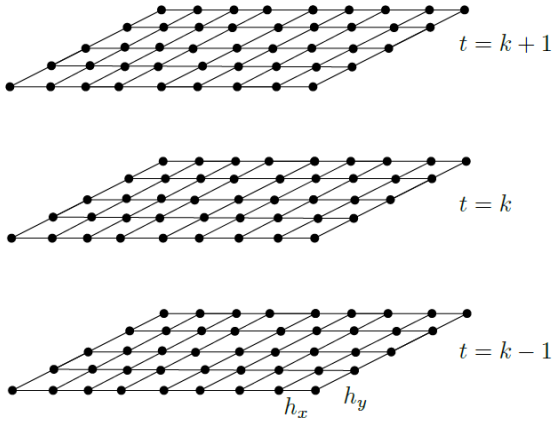

Figure 1. Space and time discretization.

Assuming $h = h_x = h_y$, λ, given by

$$\lambda = \frac{\alpha^2\tau^2}{h^2}, \tag{7}$$

and rearranging the terms of the previous equation, we obtain

$$a_p v_{i,j}^{k+1} = a_w\, v_{i-1,j}^{k+1} + a_e\, v_{i+1,j}^{k+1} + a_s\, v_{i,j-1}^{k+1} + a_n\, v_{i,j+1}^{k+1} + b_p, \tag{8}$$

where,

$$a_p = 1 + 4\eta, \tag{9}$$

$$a_w = a_e = a_s = a_n = \eta \tag{10}$$

$$b_p = \lambda\left((1-2\eta)\left(v_{i-1,j}^{k} + v_{i+1,j}^{k} + v_{i,j-1}^{k} + v_{i,j+1}^{k}\right) + \eta\left(v_{i-1,j}^{k-1} + v_{i+1,j}^{k-1} + v_{i,j-1}^{k-1} + v_{i,j+1}^{k-1}\right)\right) + \tag{11}$$

$$(2 - 4\lambda + 8\eta\,\lambda)v_{i,j}^{k} + (-1 - 4\eta\lambda)v_{i,j}^{k-1}.$$

In this case, the truncation error is given by

$$\varepsilon = \frac{\tau^4}{12}\frac{\partial^4 v_{i,j}}{\partial t^4} + \cdots - \frac{\alpha^2\,\tau_2^2\,h^2\,\eta}{12}\frac{\partial^4 v_{i,j}^{k+1}}{\partial x^4} - \cdots - \frac{\alpha^2\tau^2\,h^2}{12}(1-2\eta)\frac{\partial^4 v_{i,j}^{k}}{\partial x^4} - \cdots - \frac{\alpha^2\,\tau_2^2\,h^2\,\eta}{12}\frac{\partial^4 v_{i,j}^{k-1}}{\partial x^4} - \cdots \tag{12}$$

$$- \frac{\alpha^2\,\tau_2^2\,h^2\,\eta}{12}\frac{\partial^4 v_{i,j}^{k+1}}{\partial y^4} - \cdots - \frac{\alpha^2\tau^2\,h^2}{12}(1-2\eta)\frac{\partial^4 v_{i,j}^{k}}{\partial y^4} - \cdots - \frac{\alpha^2\,\tau_2^2\,h^2\,\eta}{12}\frac{\partial^4 v_{i,j}^{k-1}}{\partial y^4} - \cdots,$$

with truncation error order $O(h^2\tau^2, h^2\tau^2, \tau^4)$.

In order to calculate $v_{i,j}^{k+1}$, it is necessary to know the solutions of the two previous time steps, $v_{i,j}^{k}$and $v_{i,j}^{k-1}$ To initiate the process, $v_{i,j}^{k-1}$ is given by the initial setup and $v_{i,j}^{k}$is calculated with central differencing scheme by Equation (13), for more details see Burden and Faires (2016).

$$v_{i,j}^{k} = (1-\lambda)f_{i,j} + \frac{\lambda}{2}\left[f_{i,j+1} + f_{i,j-1} + f_{i+1,j} + f_{i+1,j}\right] + \tau g_{i,j} + O(h^2). \tag{13}$$

In some cases, when discretizing PDEs that model physical problems, we can obtain sparse and large linear systems as exemplified by Equation (14), which can be rewritten as

$$Au=b \tag{14}$$

These systems can be solved by using direct or iterative methods, referred to as solvers herein. Given the characteristics of these systems, direct methods become unfeasible due to their high computational cost (Burden & Faires, 2016). In such cases, we opt for iterative methods. However, these methods generally exhibit adequate smoothing properties only at the beginning of the iterative process.

After a few iterations, the approximation error becomes smooth but not necessarily small. This problem arises from the inherent nature of classical iterative methods, which quickly smooth out high frequency errors (oscillatory modes), leaving only low frequency errors (smooth modes) (Wesseling, 1995).

In this context, the Multigrid method (Brandt, 1977) can be applied. It is employed to accelerate the convergence in obtaining solutions for this type of system. By using a set of grids, it is possible to smooth both the oscillatory and smooth modes, given that the smooth modes on fine grids become more oscillatory on coarser grids (Trottenberg, Oosterlee, & Schuller, 2000). This approach allows the Multigrid iterative process to address all error components (Elman, Ernst, & O'leary, 2001).

The way it progresses through the different grid levels is referred to as cycle. In this work, we used the V-cycle, illustrated in Figure 2, which provides an example of a V-cycle for which three levels of coarsening: from fine grid Ω^h to the desired or coarsest grid Ω^{4h}. Note that we use the coarsening ratio $q = 2$, with h being the spacing in the fine grid and 2h the spacing in the immediately coarser grid.

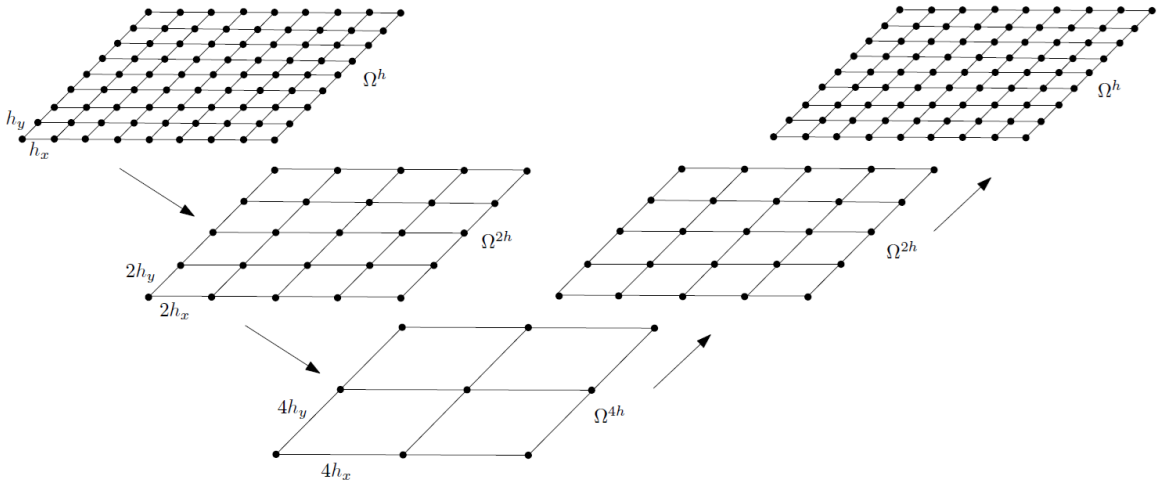

Figure 2. An example of V-cycle.

In this cycle, the system of equations is smoothed ν_1 times (pre-smoothing) on the fine grid. Afterward, we restrict its residue to the immediately coarser grid using the restriction operators $\left(I_h^{2h}\right)$. In this work, we employed the operator, given by (Trottenberg & Clees, 2009)

$$r_{2h}(x_i,y_j) = I_h^{2h}\, r_h(x_i,y_j) = \frac{1}{8}\left[4r_h(x_i,y_j) + r_h(x_{i+1},y_j) + r_h(x_{i-1},y_j) + r_h(x_i,y_{j+1}) + r_h(x_i,y_{j-1})\right] \tag{15}$$

where r_h and r_{2h} represent the residue on the fine and coarse grids, respectively. This process is repeated until the coarsest grid is reached, at which point the problem is then solved.

Next, the corrections are prolonged using the interpolation operator $\left(I_{2h}^h\right)$, as described in Trottenberg and Clees, 2009,

$$v_h(x_i,y_j) = I_{2h}^h v_{2h}(x_i,y_j) = \begin{cases} \frac{1}{2}[v_{2h}(x_{i-1},y_j) + v_{2h}(x_{i+1},y_j)], \\ \frac{1}{2}[v_{2h}(x_i,y_{j-1}) + v_{2h}(x_i,y_{j+1})], \\ \frac{1}{2}[v_{2h}(x_{i-1},y_j) + v_{2h}(x_{i+1},y_j) + \\ \quad v_{2h}(x_i,y_{j-1}) + v_{2h}(x_i,y_{j+1})], \\ v_{2h}(x_i,y_j). \end{cases} \tag{16}$$

The interpretation of the four cases of the prolongation operator can also be seen in Figure 3.

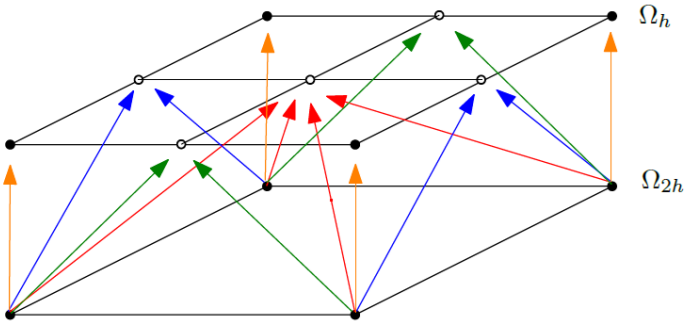

Figure 3. Where those in orange are injection interpolation, those in green and blue are linear interpolation, and those in red are bilinear interpolation.

The solution is then corrected, and the system of equations is smoothed ν_2 times (post-smoothing). This iterative process continues until the finer grid Ω^h is reached, where the solution is smoothed ν_2 times (Briggs, Henson, & McCormick, 2000; Wesseling & Oosterlee, 2001). The V-cycle is repeated until the stopping criterion is met. This approach allows for the smoothing of all error components (smooth and oscillatory) (Falgout et al., 2017).

Waveform Relaxation (WR) is an iterative method initially proposed to solve large systems of Ordinary Differential Equations (ODEs) (Lelarasmee et al., 1982). However, it can also be applied to time dependent PDEs in cases where the spatial domain is decomposed into a set of points, and for each of them, a system of ODEs is solved in all time steps (Liu & Jiang, 2011; Vandewalle, 2013). This method allows for the parallelization of algorithms for transient PDEs. The WR method transforms PDEs into an ODE system with the form,

$$\frac{d^2 v_{i,j}}{dt^2} = G_{i,j}\left(v_{i,j}, t\right), \tag{17}$$

where $G_{i,j}$ represents vectors or functions that contain temporal information foreach spatial coordinates i and j, and which is calculated with the values of $v_{i,j} = (v_{1,1}, v_{1,2}, \ldots, v_{1,d}, v_{2,1}, v_{2,2}, \ldots, v_{2,d}, \ldots, v_{d,1}, v_{d,2}, \ldots, v_{d,d})$, where d^2 is the dimension of the system. Thus, for each node $x_{i,j}$ in the spatial discretization, a temporal ODE is independently solved up to the final time. Each component of the system given in Equation (22) can be written as an ODE, as follows,

$$\begin{cases} \frac{d^2 v_{1,1}}{dt^2} = G_{1,1}\left(v_{1,1}, \ldots, v_{1,d}, \ldots, v_{d,d}, t\right) \text{ with } v_{1,1}(0) = v_{1,1}^0 \text{ and } \frac{dv_{1,1}}{dt} = g_{1,1}^0, \\ \ldots \\ \frac{d^2 v_{1,d}}{dt^2} = G_{1,d}\left(v_{1,1}, \ldots, v_{1,d}, \ldots, v_{d,d}, t\right) \text{ with } v_{1,d}(0) = v_{1,d}^0 \text{ and } \frac{dv_{1,d}}{dt} = g_{1,d}^0, \\ \frac{d^2 v_{2,1}}{dt^2} = G_{2,1}\left(v_{1,1}, \ldots, v_{1,d}, \ldots, v_{d,d}, t\right) \text{ with } v_{2,1}(0) = v_{2,1}^0 \text{ and } \frac{dv_{2,1}}{dt} = g_{2,1}^0, \\ \ldots \\ \frac{d^2 v_{2,d}}{dt^2} = G_{2,d}\left(v_{1,1}, \ldots, v_{1,d}, \ldots, v_{d,d}, t\right) \text{ with } v_{2,d}(0) = v_{2,d}^0 \text{ and } \frac{dv_{2,d}}{dt} = g_{2,d}^0, \\ \ldots \\ \frac{d^2 v_{d,d}}{dt^2} = G_{d,d}\left(v_{1,1}, \ldots, v_{1,d}, \ldots, v_{d,d}, t\right) \text{ with } v_{d,d}(0) = v_{d,d}^0 \text{ and } \frac{dv_{d,d}}{dt} = g_{d,d}^0, \end{cases} \tag{18}$$

where $1 \leq i, j \leq d$, indicate respectively, the initial configurations and velocities for each point of the spatial discretization. Each line of the system of Equations. (23) can be solved separately using a core for each line, as illustrated in Figure 4.

Each temporal EDOs must be solved independently at all spatial nodes, with theupdate of unknowns performed at the end of a WR cycle. As a result, we have aniterative method of repeating the procedure until a stopping criterion is met (Crow & Ilic, 1990). We can achieve full spatial parallelization by using a colored ordering scheme in the solver, such as red-black Gauss-Seidel (RBGS) (Vandewalle, 2013).

It is possible to combine Waveform Relaxation with the Multigrid method whenperforming coarsening only in the spatial direction because WR is continuous in time. This ensures that the number of temporal discretization points remains constant (Vandewalle, 2013). For instance, for a fine grid Ω^h with $N_x \times N_y \times N_t = 33 \times 33 \times 33$ points, the coarser grids, with a coarsening ratio $q = 2$, are $\Omega^{2h}, \Omega^{4h}, \Omega^{8h}$ and Ω^{16h}, which respectively contain $17 \times 17 \times 33, 9 \times 9 \times 33, 5 \times 5 \times 33$ and $3 \times 3 \times 33$ points. Then, a Multigrid cycle is performed at all spatial points for all time steps. The structure of the Waveform Relaxation and Multigrid approach for solving the system $A_h(t)v_h(t) = f_h(t)$.

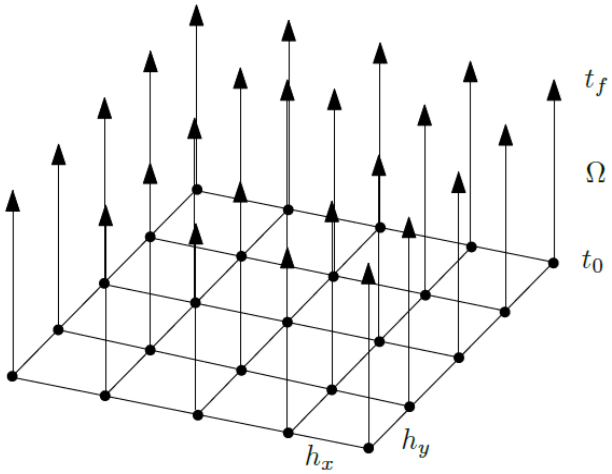

Figure 4. Standard two-dimensional Waveform Relaxation method.

In Gander, Kwok, and Mandal (2021) a variation of the Waveform Relaxation method is introduced, which can be applied to PDEs. In this approach, the domain Ω is divided into K spatial subdomains that can be independently solved until the final time, which generates a parallelizable strategy. See Figure 5 for $K = 4$.

It's worth noting that parallelization can be achieved by dedicating a processing core to each spatial subdomain. Both Gander, Kwok and Mandal (2021) and Gong, Gander, Graham, Lafontaine, Spence, and (2021) include studies to assess the stability of this approach when applied to heat and Helmholtz equations, as well as the ways of exchanging information between the subdomains. The authors also mention that at the start of the iterative process, convergence is negatively affected, and oscillations may occur in the approximate solution. However, as the iterative process advances, the solution converges to the desired values.

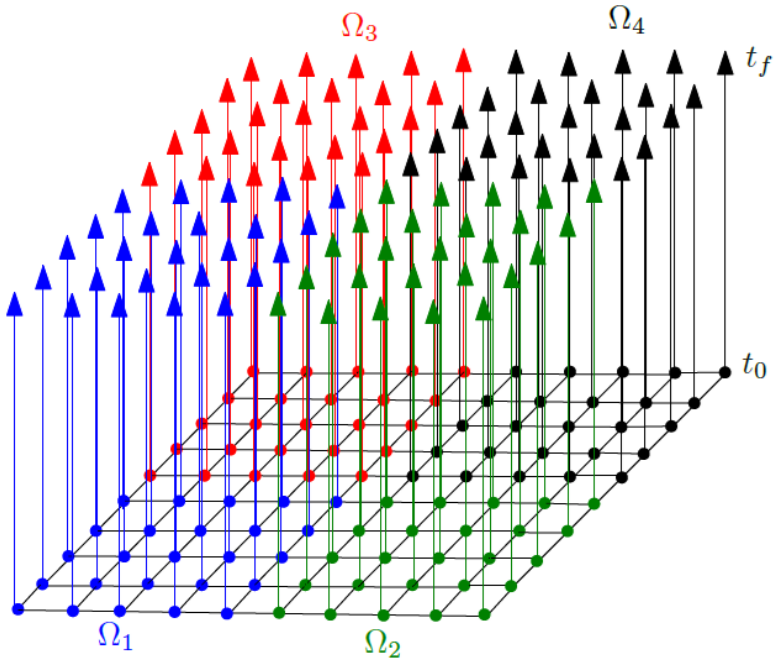

Figure 5. Division of the domain Ω into $K = 4$ subdomains.

In Gander, Kwok, and Mandal (2021) convergence is demonstrated for the one-dimensional heat transfer problem using a method called Dirichlet-Neumann Waveform Relaxation. The authors point out that the initial oscillations tend to be more pronounced when the final time is extended and/or when there are more subdomains in space. Here we face a significant challenge: while increasing the number of spatial and temporal subdomains enhances parallelization, it also tends to amplify the initial oscillations.

Another approach is proposed in Ong and Mandal (2018), where, besides the division in K spatial subdomains (see Figure 5), there is also a division in J temporal subdomains (see Figure 6). The combination of these two methods results in a highly parallelizable approach.

In Figure 6 the Waveform Relaxation method is first applied to the Ω_1 domain, whichruns from t_0 to t_{f1} . Subsequently, the solution at time t_{f1} serves as initial estimatefor the Ω_2 domain, covering the time interval from t_{f1} to t_{f2}. This process is repeateduntil the desired solution is reached, which in this example occurs at $t_{f3} = t_f$. It isimportant to note that the approach proposed in Gong et al. (2021) is a specific case of the approach presented in Ong and Mandal (2018), which adopts J = 1.

In this work, we propose an in-depth analysis of the second methodology, which employs the minimum number of spatial subdomains ($K = 1$) and a reduced number of temporal subdomains, to solve the wave equation with the WR method while mitigating the initial oscillations. To achieve this goal, we analyze the effect of parameters such as time and space intervals, physical properties of the wave, number of temporal subdomains, among others.

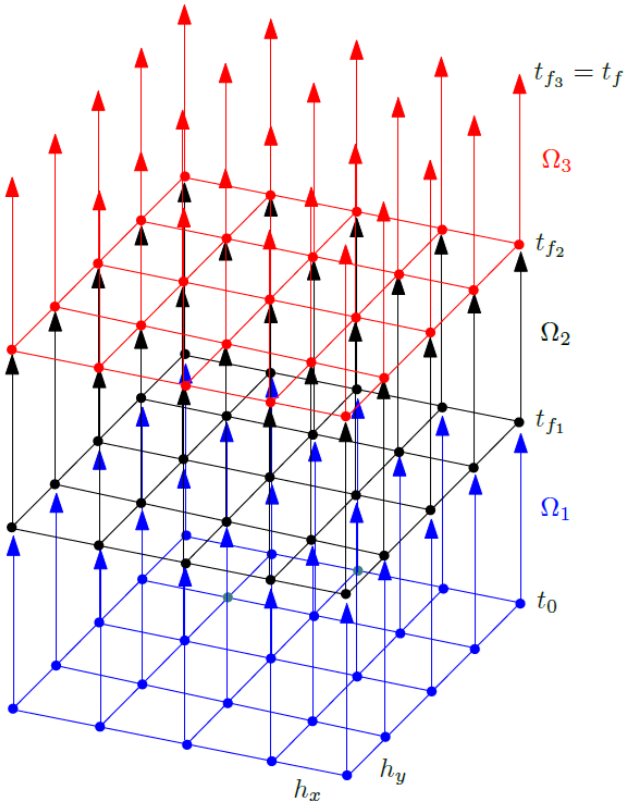

Figure 6. Subdomain method in time for J = 3.

Results and discussion

In this section, we begin by verifying the results obtained through the application of the Waveform Relaxation Method in a standard manner. This initial step confirms the limitations of this methodology, as described in Gander, Kwok, and Mandal (2021). Subsequently, we present and discuss the contributions of this work, which are achieved by combining the Waveform Relaxation strategy with the Subdomain Method in time. Solution models using Multigrid and Singlegrid Methods, average convergence factors, speedups, and processing time are also compared.

We perform the verification of the codes used, involving numericalsimulations and a posteriori analysis of the results obtained with the Multigrid and Singlegrid formulations, with standard Waveform Relaxation and combined with the Subdomain Method in time. The discretization was carried out using the Weighted Finite Difference Method with RBGS as smoother.

Discretization error

The first step is to compare the numerical solutions with the analytical solutions for the transient problem that models wave propagation over a square membrane (2D problem), described by Equations (2) to (5). This problem is solved assuming $\alpha = 2$, initial configuration $f(x, y) = sin(\pi x)sin(\pi y)$ and initial velocity

$g(x, y) = 0$. We adopt the same number of points in both spatial and temporal discretization, ie, $N = N_x = N_y = N_t$, with $\tau = h_x = h_y$, parameter $\eta = 0.5$, length $L = l_x = l_y = 1.0$ m, and final time $t_f = 1.0$ s. The choice of these parameters for verification is based on the work of Malacarne, Pinto, and Franco (2022).

The discretization error is related to the size of the grid components used (Table 1). For verifying the behavior of this type of error, in this section we neglected rounding and iteration error, considering solely the discretization error. The SG and M G represent the Singlegrid and Multigrid methods, respectively. In the first column, the number of points for the problem is N^3.

Table 1. Discretization error for different grids.

N	$\|\|E_{SG}\|\|_\infty$	$\|\|E_{MG}\|\|_\infty$
$2^3 + 1$	1.23215155E+00	1.23215155E+00
$2^4 + 1$	3.42788395E-01	3.42788395E-01
$2^5 + 1$	7.83783302E-02	7.83783302E-02
$2^6 + 1$	1.88555766E-02	1.88555766E-02
$2^7 + 1$	4.67832780E-03	4.67832780E-03
$2^8 + 1$	1.16979496E-03	1.16979494E-03
$2^9 + 1$	2.92791365E-04	2.92791376E-04

We verified a desirable characteristic in approximations: the discretization error decreases as the grid are refined. It is important to note that by adopting a certain value of N, regardless of the method used - whether it is standard Waveform Relaxation or Waveform Relaxation with Subdomains in Time (for any J), using Singledrid or Multigrid - the discretization error is virtually the same, as the problem was solved up to the rounding error. We point out that in the method of subdomains in time, the accuracy of the solution is the same for any value of J. In contrast to Malacarne, Pinto, and Franco (2022), in this work we use the Waveform Relaxation method and its variations with the Subdomains in Time.

Effective and apparent orders

Studies that explore methodologies for qualitatively verifying numerical solutions are valuable in various fields of computer simulation. In Da Silva, Rutyna, Righi, and Pinto (2021), the authors showed how to use the effective P_e and apparent P_u order of accuracy to assess the coherence of numerical solutions in computational heat transfer problems. Notably, in Da Silva, Marchi, Meneguette, and Foltran, 2022, the authors confirmed the robustness of this methodology, showing its applicability even in discretization that do not use meshes, for example, using the SPH method. The advantage of the apparent order of accuracy lies in the fact that the analytical solution may be unknown, and numerical error analyzes are shown in Da Silva et al., (2021) for several cases. In this work, we apply to the Richardson estimator based on the effective and apparent orders of numerical error. The results are presented in Table 2.

Table 2. Apparent and effective orders.

h	P_u	P_e
1/8	1.75002700E+00	1.84580825E+00
1/16	2.15123967E+00	2.12877283E+00
1/32	2.06986367E+00	2.05546357E+00
1/64	2.01463782E+00	2.01092641E+00
1/128	2.00021321E+00	1.999737269E+00
1/256	1.999816227E+00	1.998755489E+00
1/512	-	1.998310716E+00

The results indicate that the method employed in this work exhibits apparent and effective orders tending to asymptotic order $p_L = 2$. These findings are aligned with the literature in the work of Malacarne, Pinto and Franco (2022), where the Time-Stepping method was employed. These results validate our solution methodology, using Standard Waveform Relaxation and Waveform Relaxation with Subdomains in Time.

Standard waveform relaxation

In this section, we demonstrate the oscillatory behavior of the solution during the iteration, using the standard Waveform Relaxation method. To do so, we solve a two-dimensional problem modeled by Equations

(2) to (5), using Singlegrid (SG) and Gauss Seidel with Red Black ordering as the solver, on a grid with $N = 129$, ie, 129^3 total number of points. Figure 7 and Figure 8 depict the solutions for the profile at $y = 0.5\,m$, after 5 and 50 iterations, and Figure 9 and Figure 10 display the solutions after 200 and 1500 iteration, both using final time $t_f = 1.0\,s$.

Remark: In the range of Figures 7 to 9, due to the scale, the configuration of the analytical solution is not visible. However, as the iterations progress, convergence occurs, and this configuration becomes evident, as shown in Figure 10. The analytical solution is obtained directly.

We verified significant initial oscillations when applying the standard Waveform Relaxation method, even when using coarser grids (with fewer points). Despite the pronounced oscillation at the beginning of the process, the numerical solution converges with the desired values as the number of iterations increases.

In Figure 11 it is possible to observe the behavior of the infinity norm of the residue as the iterations are performed, using Singlegrid method and standard Waveform Re- laxation method.

The initial oscillations lead to increased error in the approximate solutions whichis an undesirable characteristic in the approximation process. Although it is well-documented in the literature, the causes of this increase remain unknown and negatively impact the convergence factors and CPU time (Gander, Kwok, & Mandal, 2021). By using the Multigrid method, we are not able to reduce the order of the residue; despite performing fewer cycles, the order of perturbation of the residue is the same.

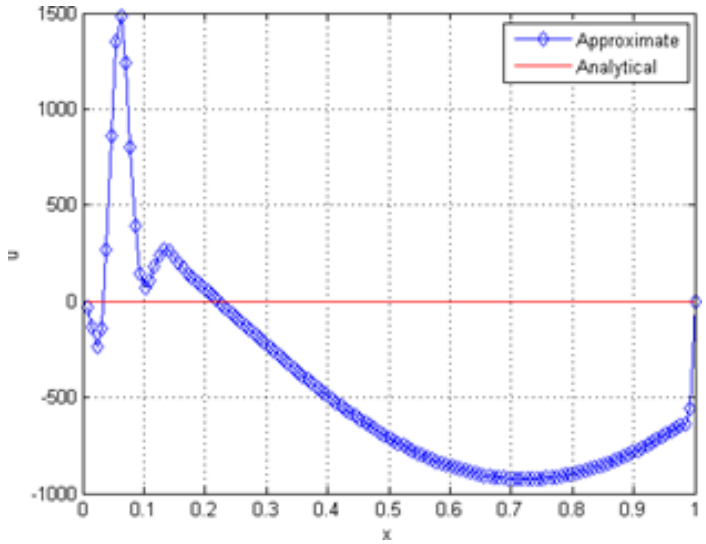

Figure 7. Solution with 5 iterations.

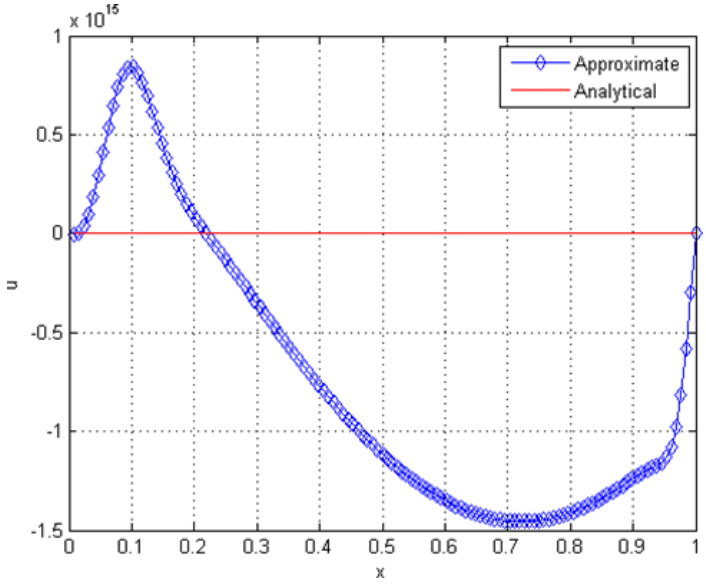

Figure 8. Solution with 50 iterations.

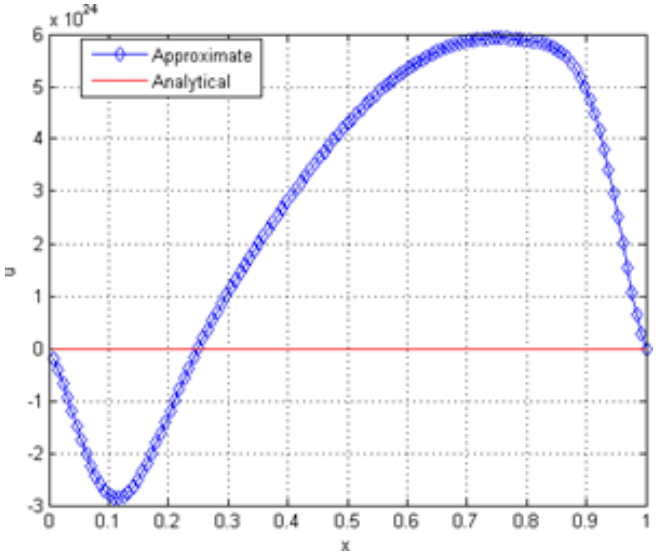

Figure 9. Solution with 200 iterations.

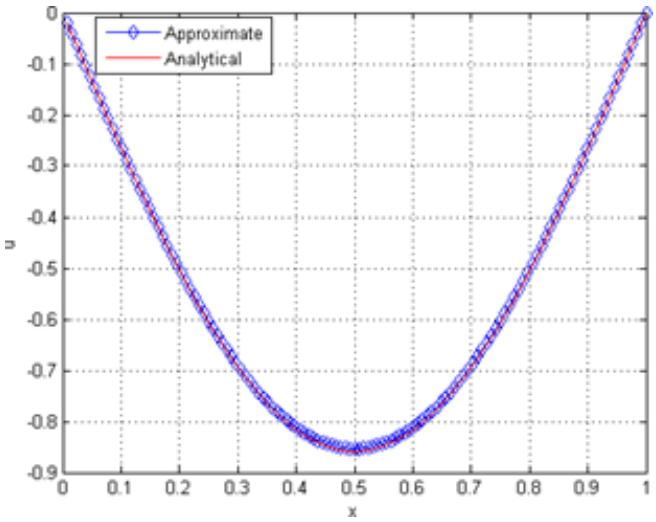

Figure 10. Solution with 1500 iterations.

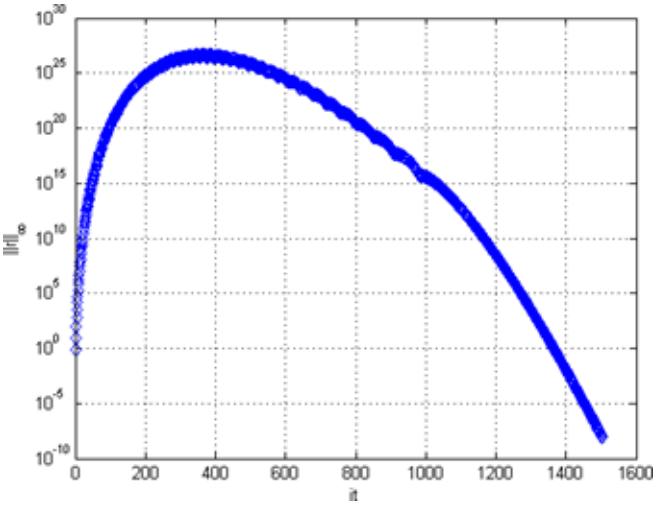

Figure 11. Residue *versus* iterations for Singlegrid with standard Waveform Relaxation

Average convergence factor for Waveform Relaxation

In this section, we apply the standard Waveform Relaxation method to the problem described in the previous section, varying final time. To do so, let the convergence factor be $\rho = ||r^{it}||_\infty / ||r^{it-1}||_\infty$, with r^{it}

being the residue generated in the iteration it. A value of $\rho \approx 0$ results in more efficient methods, while $\rho \approx 1$ means the opposite (Briggs et al., 2000) $\rho \approx 1$ means that with each new iteration, the improvement in the approximate solution is almost imperceptible). We also define the average convergence factor ρ_m (Trottenberg & Clees, 2009), given by

$$\rho_m = \sqrt[it]{\frac{||r^{it}||_\infty}{||r^0||_\infty}} \tag{19}$$

According to Vandewalle and Horton (1993) $\lambda = \alpha^2\tau^2/h^2$ can be considered a measure of the anisotropy level in the discretized operator within a given grid. Such anisotropy can impact the performance of the solver. As λ depends on the temporal and spatial increments adopted in the discretization and on the velocity of the propagation of the wave, λ thus represents a measure of physical and geometrical anisotropy of the wave equation.

We can express the final time depending directly on λ and α, using the expression$t_f = \sqrt{\lambda}/\alpha$. Then, we present the test results where we vary the parameter λ andcalculate ρ_m for a wide range of problems, covering most real cases of wavepropagation. To verify the behavior of the standard Waveform Relaxation method using the Singlegrid and Multigrid Methods, see Figure 12.

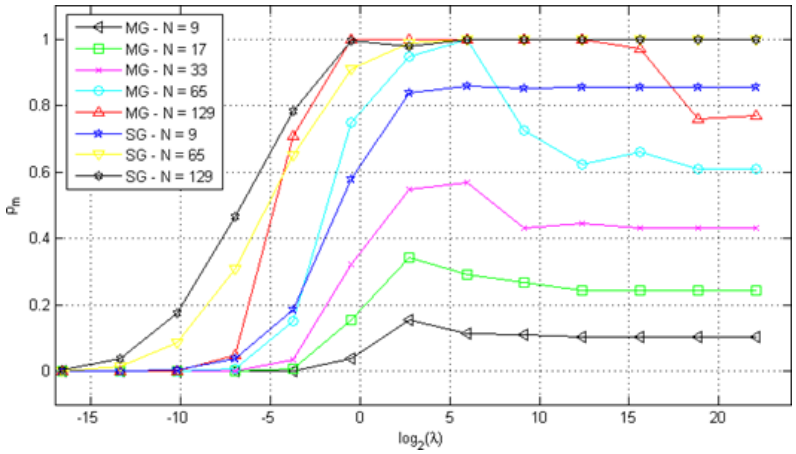

Figure 12. ρ_m *versus* λ with standard Waveform Relaxation using Multigrid and Singlegrid.

As observed in Figure 12, as λ increases, the average convergence factors of the Multigrid and Singlegrid Methods also increase, becoming $\rho_m \approx 1.0$, which is not favorable. Consequently, we conclude that the solution model is neither efficient nor robust for intermediate or large λ values (cases with many unkwows and longer final times). This result supports the hypothesis that it is inefficient to apply the standard Waveform Relaxation method to solve the wave equation, whether using the Multigrid or Singlegrid methods.

The hyperbolic transient wave computational simulation problem can be solved in different ways, but most of these approaches have limitations, especially for relatively large final times. In such cases, explicit schemes exhibit instabilities that compromise the reliability of the approximate solution (Bailly & Juve, 2000). As observed, even implicit methods present difficulties in solving these cases, because at the beginning of the iterative process, the approximate solutions present strong oscillations, which are smoothed out as the number of iterations increases (see Figure 7 and 9). However, this significantly affects the efficiency of such methods. Therefore, we aim to enhance the applicability of parallelizable methods, such as the Waveform Relaxation Method. To achieve this, we combine the methodologies developed so far with the Subdomains in Time method, as illustrated in Figure 6.

Waveform relaxation with subdomain in time

From this section on, we present the results of the Waveform Relaxation Method combined with the Subdomain in time method. For this analysis, set $K = 1$ for the number of spatial subdomains. Regarding the number J of subdomains in time, we choose the smallest possible value that can provide satisfactory average convergence factors (ρ_m). In Table 1 are the values used for J, which may vary depending on the values of $N^3 = N_x N_y N_t$ and λ. It is important to note that numerous simulations were conducted, exploring various combinations in the number of subdomains, where the choice of J was based on empirical analysis of this data.

The results present in Table 3 were chosen to achieve an average convergence factor of $\rho_m \approx 0.4$ or less. This criterion is used to determine the acceptability of the implicit numerical model (Trottenberg & Clees,

2009). We should also note that, for large J, the number of spatial meshes within each temporal subdomain will be small, which may reduce the level of parallelization of the method. Therefore, it is always advantageous to have the smallest possible value for J, but in the case of J $=$ 1, we have the standard Waveform Relaxation method, which we already know is inefficient.

Table 3. Number J of subdomain in time according to the ranging of N^3 and λ.

$N^3 \backslash \lambda$	10^{-2}	10^{-1}	10^{0}	10^{1}	10^{2}	10^{3}	10^{4}	10^{5}	10^{6}	10^{7}
9^3	1	1	1	2	2	2	2	2	2	2
17^3	1	1	2	2	2	2	2	2	2	2
33^3	1	1	2	2	2	2	2	2	2	2
65^3	1	1	4	4	4	4	4	4	4	4
129^3	1	2	8	8	8	8	8	8	8	8
257^3	1	4	8	16	16	16	16	16	16	16

It is also possible to notice that for domains with small N, the largest number of subdomains in time are J $=$ 2, regardless of the value of λ. However, for problems with large N, the choice of J depends on λ since very small values of J can lead to instabilities in the standard Waveform Relaxation technique, negatively impacting the values of ρ_m. Looking at Tab. 3, we can state that it is necessary to work with at most 16 spatial meshes within each temporal subdomain to ensure efficient solving (see Figure 13).

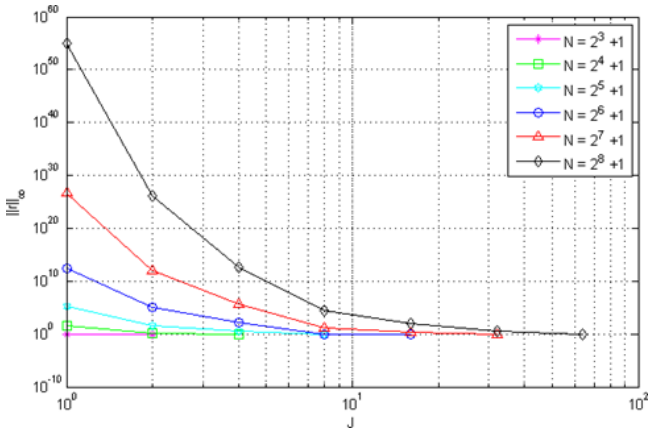

Figure 13. Residue *versus* J, for $t_f = 1.0\ s$ and $K = 1$, varying N, with Singledrid and Waveform Relaxation with Subdomain in Time.

In Figure 13 we depict the behavior of the maximum residue order concerning thenumber of temporal subdomains J, as well as the values of N, considering $K = 1$. We also solved the example of Figures 7 to 9 using Waveform Relaxation Method withSubdomain in Time (for J $=$ 8). Figure 14 and 15 presents the solutions for the profile on the $y = 0.5m$, for 5 and 50 iterations, and Figure 16 displays the solutions for 200 iterations.

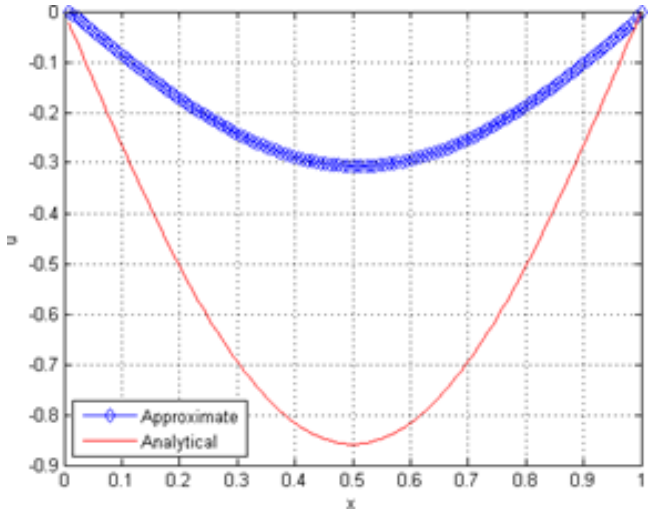

Figure 14. Solution with 5 iterations.

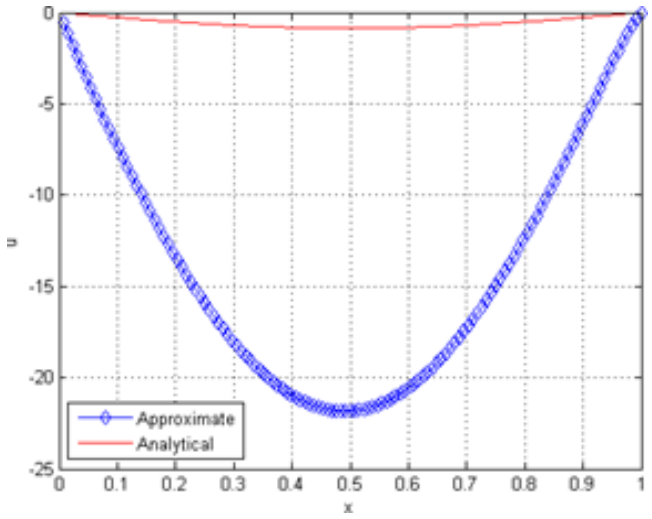

Figure 15. Solution with 50 iterations.

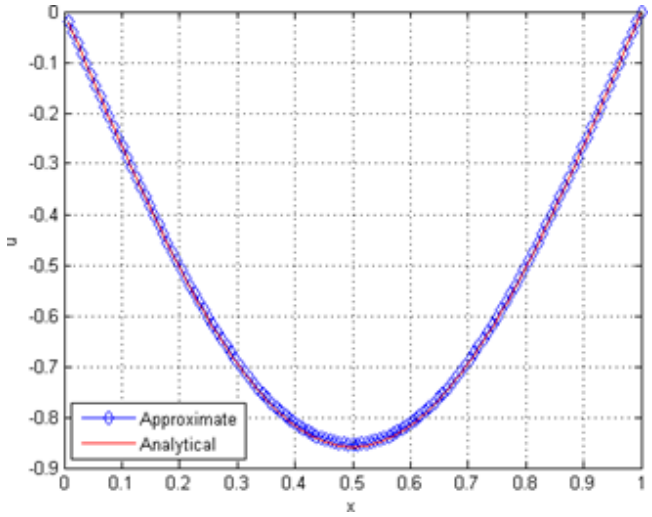

Figure 16. Solution with 200 iterations.

We found that the initial oscillations were significantly reduced when using the Waveform Relaxation Method with the Subdomain in Time, requiring fewer iterations to approach the analytical solution. The number of iterations performed with Singlegrid is lower here, approximately 241 *versus* 1510 iterations when using standard Waveform Relaxation. Furthermore, the residue is on the order of 10^{1} (see Figure 17), smaller than the 10^{26} that was obtained in the Figure 11.

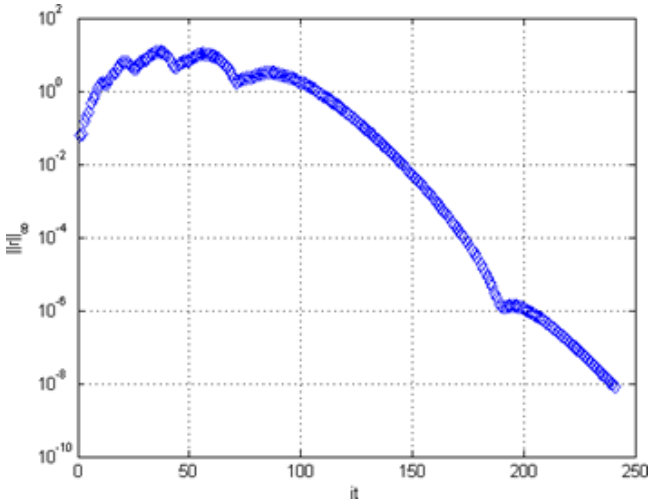

Figure 17. Residue *versus* iterations for Singlegrid with Waveform Relaxation Subdomain in Time (for J = 8).

Average convergence factor for waveform relaxation with subdomain in time

In Figure 18 we present the results obtained for ρ_m when applying the Waveform Relaxation method with subdomains in time, with Multigrid and Singlegrid, for the same range of problems described previously in this work.

It is worth noticing that unlike in Figure 12, in Figure 18 the ρ_m values of the Multigridmethod tend to stabilize $\rho_m \approx 0.35$, as λ and N increase. These results demonstratethe efficiency and robustness of Multigrid. We also notice that the average convergence factors of the Singlegrid method remain close to unity $\rho_m \approx 1.0$ as λ and N increase.

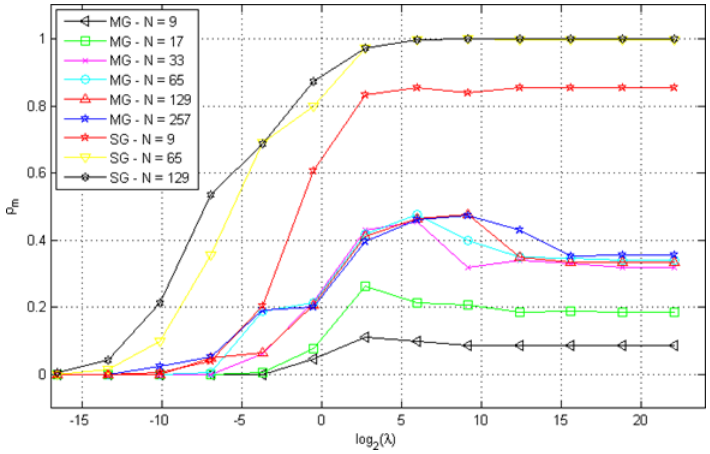

Figure 18. ρ_m *versus* λ with Waveform Relaxation with Subdomain in time.

The number of subdomains used in Figure 18 can be found in Tab. 1, where we observe larger values of J when working with large N and λ. Additionally, we can observe that for intermediate λ values, we have the worst ρ_m values for the Multigrid method, but in general, they are smaller than those achieved with the Singlegrid method.

Speedup

Next, we examine the relationship between the computational time of the Singlegrid(T_{cpuSG}) and Multigrid (T_{cpuMG}) and the increase in the number of points, wherethe $Speedup = T_{cpuSG})/T_{cpuMG})$. See Figure 19, for different values of λ. We adopted the total numbers of unknowns (U) as the total number of inner unknowns, excluding boundary points.

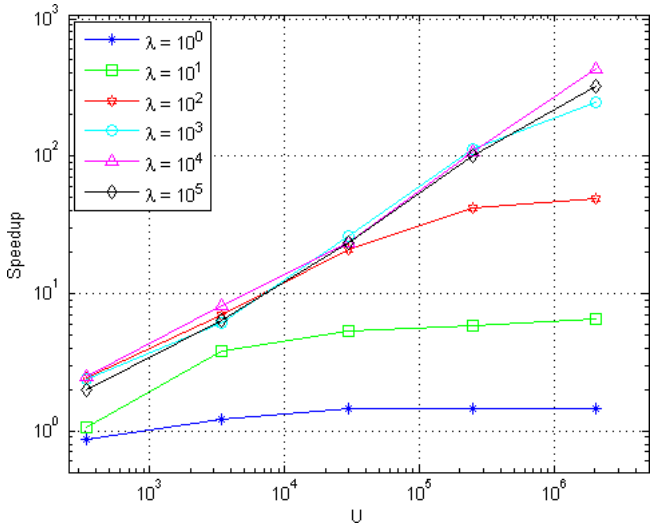

Figure 19. Speedup *versus* total numbers of unknowns.

We observed that for all cases, the Speedup increases with higher values of U, which is desirable property, and it significantly increases with higher values of λ. For example, with $\lambda = 10^1$ and $N = 129$, that is, with 2146689 points and 2048383 total numbers of unknowns, using the Multigrid method, we have $T_{cpuMG} = 455.19$ s for J = 1 and $T_{cpuMG} = 80.78$ s for J = 8. In this case, the maximum residue decreases from 5.19E+27 for 2.39E+03.

When the same example is solved using Singledrid method, we observe similar orders for the maximum residue, but the computational time changes from $T_{cpuMG} = 2447.46$ s to $T_{cpuSG} = 495.29$ s. In other words, by using the Multigrid method with J = 8, we solve the problem approximately 30 times faster than with Singlegrid with J = 1. Looking at Figure 19, we can see that this difference between the Multigrid and Singlegrid methods become more pronounced for larger N or λ.

As another example, with $\lambda = 10^5$, N = 129 and J = 1, using the Multigrid method, we have $T_{cpuMG} = 222.68$ s while using the Singlegrid method, we have $T_{cpuSG} = 26262.72$ s. This means that we obtain the same solution approximately 122 times faster when using Multigrid method. This result is even more favorable for J = 8 since in, this case Multigrid solves the problem 381 times faster. In the next section we will present the analysis of the effects of each method separately.

Other comparisons

Up to this point, we have seen that the combination of the Subdomains method with the Multigrid method yields excellent results. However, which of these methods has the greatest impact on this improvement? To answer this question, we present the results for the maximum residue $||r||_\infty$, processing time T_{cpu}, and average convergence factor ρ_m in Table 4. Here, we keep $\lambda = 10^1$, $N = 129$ and vary the J number of subdomains. The N adopted here generates a relatively large problem.

Table 4. Multigrid and Singlegrid with Subdomain method with Waveform Relaxation for $\lambda = 10^1$ and N = 129.

J	T_{cpuSG}	T_{cpuMG}	$\|\|r\|\|_\infty$	ρ_{m-SG}	ρ_{m-MG}
1	2447.46s	455.19s	5.19E+27	9.997E-01	9.994E-01
2	1324.46s	214.58s	7.10E+13	9.904E-01	9.224E-01
4	768.75s	120.05s	1.09E+06	9.827E-01	6.027E-01
8	495.29s	80.78s	2.39E+03	9.718E-01	4.133E-01
16	351.34s	61.18s	8.70E+01	9.565E-01	2.149E-01

In Table 4, we can verify the interference of the number of subdomains on the threeparameters analyzed for both methods (Multigrid and Singlegrid). We observed that the maximum residual $||r||_\infty$ went from 5.19E+27 with J = 1, to 8.70E+01 with J = 16. There is also a reduction in the average convergence factors ρ_m, although this reduction is less evident in the Singlegrid method, going from 9.997E-01 to 9.565E-01. For the Multigrid method, the reduction is more significant, going from 9.994E-01 to 2.149E-01. The processing time T_{cpu} decreases significantly as the number of subdomains increases, going from 2447.46 s to 351.34 s with Singlegrid and from 455.19 s to 61.18 s with Multigrid.

As we have observed earlier, for problems with large N, we use large values for λ to refine spatial meshes or extend final times. Therefore, we solved the same problemgiven by Table 4, but now using $\lambda = 10^5$, as shown in Table 5.

Table 5. Multigrid and Singlegrid with Subdomain method with Waveform Relaxation for $\lambda = 10^5$ and $N = 129$.

J	T_{cpuSG}	T_{cpuMG}	$\|\|r\|\|_\infty$	ρ_{m-SG}	ρ_{m-MG}
1	26262.72s	222.68s	3.627E+03	9.995E-01	7.958E-01
2	23751.65s	132.95s	3.627E+03	9.994E-01	6.748E-01
4	22920.39s	87.15s	3.627E+03	9.994E-01	5.047E-01
8	21695.46s	68.87s	3.627E+03	9.993E-01	3.354E-01
16	25469.29s	61.10s	3.627E+03	9.993E-01	2.038E-01

We observe in Table 3 that the difference between the Multigrid and Singlegridmethods is even more pronounced $\lambda = 10^5$. In this case, there was no decrease in the maximum residual, but the values are not as large as those presented in Table 2. In this case, the reduction of the average convergence factors of the Singlegrid method is almost negligible, going from 9.995E-01 to 9.993E-01. In contrast, for the Multigrid method, this parameter goes from 7.958E-01 to 2.038E-01. With $\lambda = 10^5$, the processing time of the Singlegrid method does not change to the same extent as it did in the case where $\lambda = 10^1$.

However, the Multigrid method still exhibits similar behavior in both cases. This indicates that the Subdomains method, when applied without the Multigrid method, is not so efficient for the problems addressed in this work. However, when the two methods are combined, we have an excellent solution method for the wave propagation problem. We can see this by looking at the processing time of the Singlegrid method

which changes from 26262.72 s to 25469.29 s, while the processing time of the Multigrid method goes from 222.68 s to 61.10 s. This represents an approximate difference of up to 423 times faster when using the Multigrid method compared to Singlegrid.

Conclusion

In this study, we conducted a series of tests and comparisons between Multigrid andSinglegrid methods while employing both the parallelizable standard Waveform Relaxation and Waveform Relaxation with Subdomains in Time to solve two-dimensional wave propagation problems. The results obtained with standard Waveform Relaxation revealed substantial limitations, due to an increase in oscillations at the beginning of the iterative process, resulting in an inefficient approach for this class of problems. It is also important to highlight that applying the Multigrid method without the Subdomains in time leads to limited improvements. Equally inefficient results are obtained if the Subdomains in time method is applied without the Multigrid method, indicating a strong interdependence between these methods. We emphasize that the key innovation of this work lies in the combination of the Waveform Relaxation with Subdomains in Time and the Multigrid methods. This integration has significantly produced improvements in the parameters analyzed, especially in terms of average convergence factors, speedups, and reduction of initial oscillations, which have led to a substantial decrease in processing time.

References

Bailly, C., & Juve, D. (2000). Numerical solutions of acoustic propagation problems using linearized Euler equations. *AIAA journa*l, *38*, 22-29.

Bellen, A., & Zennaro, M. (1989). Parallel algorithms for initial-value problems for difference and differential equations. *Journal of Computational and applied mathematics*, *25*(3), 341-350. DOI: https://doi.org/10.1016/0377-0427(89)90037-X

Benedusi, P., Minion, M. L., & Krause, R. (2021). An experimental comparison of a Space-Time Multigrid method with PFASST for a reaction-diffusion problem. *Computers and Mathematics with Applications*, *99*, 162-170. DOI: https://doi.org/10.1016/j.camwa.2021.07.008

Bolten, M., Moser, D., & Speck, R. (2017). A Multigrid perspective on the parallel full approximation scheme in space and time. *Numerical Linear Algebra with Applications*, *24*(6), e2097-e2110. DOI: https://doi.org/10.1002/nla.2110

Brandt, A. (1977), Multi-level adaptive solutions to boundary-value problems. *Mathematics of Computation*, *78*, 333-390. DOI: https://doi.org/10.1090/S0025-5718-1977-0431719-X

Briggs, W. L., Henson, V. E., & McCormick, S. F. (2000). *A Multigrid tutorial* (2nd ed.) Philadelphia, PA: SIAM.

Burden, R., & Faires, J. (2016). *Numerical analysis*. Brooks/Cole Cengage Learning.

Chartier, P., & Philippe, B. (1993). A parallel shooting technique for solving dissipative ODE's. *Computing*, *51*, 209-236. DOI: https://doi.org/10.1007/BF02238534

Conte, D., D'Ambrosio, R., & Paternoster, B. (2016). GPU-acceleration of waveform relaxation methods for large differential systems. *Computational and Applied Mathematics*, *71*, 293-310. DOI: https://doi.org/10.1007/s11075-015-9993-6

Crow, M. L., & Ilic, M. (1990). The parallel implementation of the Waveform Relaxation method for transient stability simulations. *Transactions on Power Systems*, *5*(3), 922-932.

Da Silva, L. P., Marchi, C. H., Meneguette, M., & Foltran, A. C. (2022). Ro-bust RRE technique for increasing the order of accuracy of SPH numerical solutions. *Mathematics and Computers in Simulation*, *199*, 231-252. Doi: https://doi.org/10.1016/j.matcom.2022.03.016

Da Silva, L. P., Rutyna, B. B., Righi, A. R. S., & Pinto, M. A. V. (2021). High Order of Accuracy for Poisson Equation Obtained by Grouping of Repeated Richardson Extrapolation with Fourth Order Schemes. *Computer Modeling in Engineering and Sciences*, *128*(2), DOI: https://doi.org/10.32604/cmes.2021.014239

Dai, X., & Maday, Y. (2013). Stable parareal in time method for first-and second order hyperolic systems. *Journal on Scientific Computing*, *35*, A52-A78. DOI: https://doi.org/10.1137/11086100

De Oliveira, F., Franco, S. R., & Pinto, M. A. V. (2018). The effect of Multigrid parameters in a 3D heat diffusion equation. *International Journal of Applied Mechanics and Engineering*, *23*, 213-221. Doi: https://doi.org/10.1515/ijame-2018-0012

Dobrev, V. A., Kolev, T., Petersson, N. A., & Schroder, J. B. (2017). Two-level convergence theory for Multigrid reduction in time MGRIT, Journal on Scientific Computing, *39*(5)*,* S501-S527. DOI: https://doi.org/10.1137/16M1074096

Elman, H. C., Ernst, O. G., & O'leary, D. P. (2001). A Multigrid method enhanced by Krylov subspace iteration for discrete Helmholtz equations. *Journal on scientific computing*. *23*(4), 1291-1315. DOI: https://doi.org/10.1137/S1064827501357190

Falgout, R. D., Friedhoff, S., Kolev, T. V., MacLachlan, S. P., & Schroder, J. B. (2014). Parallel time integration with Multigrid. *Journal on Scientific Computing*, *36*(6), C635-C661. DOI: https://doi.org/10.1137/130944230

Falgout, R. D., Friedhoff, S., Kolev, T. V., MacLachlan, S. P., Schroder, J. B., & Vandewalle, S. (2017). Multigrid methods with Space–Time concurrency. *Computing and Visualization in Science*, *18*, 123-143. DOI: https://doi.org/10.1007/s00791-017-0283-9

Foltyn, L., Lukas, D., & Peterek, I. (2020). Domain decomposition methods cou-pled with parareal for the transient heat equation in 1 and 2 spatial dimen-sions. *Applications of Mathematics*, *65*(2), 173-190. DOI: https://doi.org/10.21136/AM.2020.0219-19

Franco, S. R., Gaspar, F. J., Pinto, M. A. V., & Rodrigo, C. (2018a). Multigrid method based on a Space-Time approach with standard coarsening for parabolic prob-lems. *Applied Mathematics and Computation*, *317*, 25-34. DOI: http://dx.doi.org/10.1016/j.amc.2017.08.043 identificar no texto

Franco, S. R., Rodrigo, C., Gaspar, F. J., & Pinto, M. A. V. (2018b). A Multigrid Waveform Relaxation method for solving the poroelasticity equations. *Computational and Applied Mathematics*, *37*, 4805-4820. DOI: https://doi.org/10.1007/s40314-018-0603-9

Franco, S. R., & Pinto, M. A. V. (2023). A space-time multigrid method for poroelasticity equations with random hydraulic conductivity. Numerical Heat Transfer. *Fundamentals*, *Part B*, *85(9)*, 1226-1235. DOI: https://doi.org/10.1080/10407790.2023.2262746

Gander, M. J. (2015). 50 Years of Time Parallel Time Integration. *Springer International Publishing*, *51*, 69-113. DOI: https://doi.org/10.1007/978-3-319-23321-53

Gander, M. J., Halpern, L., Rannou, J., & Ryan, J. (2019), A direct time parallel solver by diagonalization for the wave equation. *Journal on Scientific Computing*, *41,* A220-A245.

Gander, M. J., Kwok, F., & Mandal, B. C. (2021). Dirichlet–Neumann Waveform Relaxation methods for parabolic and hyperbolic problems in multiple subdomains. *BIT Numerical Mathematics*, *61*, 173-207. DOI: https://doi.org/10.1007/s10543-020-00823-2

Gander, M. J., & Neumuller, M. (2016). Analysis of a new Space-Time parallel Multigrid algorithm for parabolic problems. *Journal on Scientific Computing*, *38*(4), A2173-A2208. DOI: https://doi.org/10.1137/15M1046605

Giladi, E., & Keller, H. B. (2002). Space-Time domain decomposition for parabolic problems. *Numerische Mathematik*, *93*, 279-313. DOI: https://doi.org/10.1007/s002110100345

Gong, S., Gander, M. J., Graham, I. G., Lafontaine, D., & Spence, E. A. (2021). Convergence of parallel overlapping domain decomposition methods for the Helmholtz equation. *Numerical Analysis*, 1*52*, 259-306. DOI: https://doi.org/arXiv:2106.052180

Haut, T. S., Babb, T., Martinsson, P. G., & Wingate, B. A. (2016). Direct construction of an approximate time-evolution operator. *IMA Journal of Numerical Analysis*, *36*(2), 688-716. DOI: https://doi.org/10.1093/imanum/drv021

Keller, H. B. (1992). Numerical methods for two-point boundary-value problems. New York, NY: Courier Dover Publications.

Klaij, C. M., Van Der Vegt, J. W., & van der Ven, H. (2006). Space–Time discontinuous Galerkin method for the compressible Navier–Stokes equations. *Journal of Computational Physics*, *217*(2)*,* 589-611. DOI: https://doi.org/10.1016/j.jcp.2006.01.018

Kocher, U., & Bause, M. (2014). Variational Space–Time methods for the wave equa-tion. *Journal of Scientific Computing*, *61*(2), 424-453. DOI: https://doi.org/10.1007/s10915-014-9831-3

Lelarasmee, E., Ruehli, A. E., & Vincentelli, S. A. L. (1982). The Waveform Relaxation Method for Time Domain Analysis of Large-Scale Integrated Circuits Theory and Apllications. *Journals and Magazines*, *1*(3), 131-145. DOI: https://doi.org/10.1109/TCAD.1982.1270004

Liu, J., & Jiang, Y. L. (2011). Waveform Relaxation for reaction–diffusion equations. *Journal of Computational and Applied Mathematics*, *235*(17), 5040-5055. DOI: https://doi.org/10.1016/j.cam.2011.04.035

Malacarne, M. F., Pinto, M. A. V., & Franco, S. R. (2022). Performance of the Multigrid method with Time-Stepping to solve 1D and 2D wave equations. *International Journal for Computational Methods in Engineering Science and Mechanics*, *23*, 45-56. DOI: https://doi.org/10.1080/15502287.2021.1910750

Nguyen, H., & Tsai, R. (2020). A stable parareal-like method for the second order wave equation. *Journal of Computational Physics*, *405*, 109-156. DOI: https://doi.org/10.1016/j.jcp.2019.109156

Olver, P. J. (2014). Introduction to partial differential equations. Berlin, DE: Springer.

Ong, B. W., & Mandal, B. C. (2018). Pipeline implementations of Neumann–Neumann and Dirichlet–Neumann Waveform Relaxation methods. *Numerical Algorithms*, *78*, 1-20. DOI: https://doi.org/10.1007/s11075-017-0364-3

Ong, B. W., & Schroder, J. B. (2020). Applications of time parallelization. *Computing and Visualization in Science*, *23*(11), 1-15. DOI: https://doi.org/10.1007/s00791-020-00331-4

Pierce, A. D. (1990). Wave equation for sound in fluids with unsteady inhomogeneous flow. *The Journal of the Acoustical Society of America*, *87*, 2292-2299.

Pinto, M. A. V., Rodrigo, C., Gaspar, F. J., & Oosterlee, C. W. (2016). On the robustness of ILU smoothers on triangular grids. *Applied Numerical Mathematics*, *106*, 37-52. DOI: https://doi.org/10.1016/j.apnum.2016.02.007

Rodrigues, S., Pinto, M. A. V., Martins, M. A., & Franco, S. R. (2022). Reducing the discretization error for a poroelasticity problem in variables having extreme values. *Journal of the Brazilian Society of Mechanical Sciences and Engineering*, *44*(147), 1-11. DOI: https://doi.org/10.1007/s40430-022-03410-4

Ruprecht, D. (2018). Wave propagation characteristics of parareal. *Computing and Visualization in Science*, *19,* 1-17. DOI: https://doi.org/10.1007/s00791-018-0296-z

Trottenberg, U., & Clees, T. (2009). Multigrid software for industrial applications-from MG00 to SAMG. *Journal on scientific computing*, *100*, 423-436.

Trottenberg, U., Oosterlee, C. W., & Schuller, A. (2000), *Multigrid*. London, UK; California, US: Elsevier - Academic Press.

Vandewalle, S. (2013). Parallel Multigrid Waveform Relaxation for parabolic problems. Stuttgar, DE: Springer-Verlag.

Wesseling, P. (1995). *Introduction to Multigrid methods*. NASA-CR-195045.

Wesseling, P., & Oosterlee, C. (2001). Multigrid with Applications to Computational Fluid Dynamics. *Journal of Computational and Applied Mathematics, 128*, 311-334.